Available online at www.sciencedirect.com

SCIENCE DIRECT®

Journal of Solid State Chemistry 177 (2004) 3080–3085

JOURNAL OF SOLID STATE CHEMISTRY

http://elsevier.com/locate/jssc

Syntheses, crystal structures and magnetic properties of two new bimetallic phosphates $M(\text{phen})(H_2O)(VO)(H_2O)(HPO_4)_2$ ($M = $ Ni, Co; phen = 1,10-phenanthroline)

Yanjie Cui, Yan Xing, Guanghua Li, Yunling Liu, He Meng, Li Liu, and Wenqin Pang*

State Key Laboratory of Inorganic Synthesis and Preparative Chemistry, College of Chemistry, Jilin University, Changchun 130012, People's Republic of China

Received 18 November 2003; received in revised form 28 April 2004; accepted 30 April 2004

Abstract

Two novel layered organic–inorganic hybrid materials $M(\text{phen})(H_2O)(VO)(H_2O)(HPO_4)_2$ ($M = $ Ni, Co) have been synthesized hydrothermally, their crystal structures and variable temperature magnetic susceptibilities were determined. Being characterized by single-crystal X-ray diffraction, the two compounds are isostructural and crystallize in the monoclinic system with $P2_1/c$ space group with $a = 14.3903(7)$ Å, $b = 15.5232(6)$ Å, $c = 7.3943(3)$ Å, $\beta = 90.577(2)^\circ$, $Z = 4$, $V = 1651.7(2)$ Å^3 and $R_1 = 0.0358$ for **1**, and $a = 14.3726(4)$ Å, $b = 15.5078(5)$ Å, $c = 7.3932(2)$ Å, $\beta = 90.576(2)^\circ$, $Z = 4$, $V = 1647.77(8)$ Å^3 and $R_1 = 0.0323$ for **2**. The structure exhibits an unusual 4,12-membered rings oxovanadium phosphate (V–P–O) layer capped by $[M(\text{phen})]^{2+}$ complexes with phen groups projecting above and below into the interlamellar regions. Therefore, the bimetallic phosphate undulating layers extend into three-dimensional supermolecular arrays through a strong $\pi-\pi$ stacking interaction of the phen groups between adjacent layers.

Keywords: Hydrothermal synthesis; 1,10-phenanthroline; Organic–inorganic hybrid material; Magnetic property; Layer; Nickel/cobalt–vanadium phosphate; Crystal structure

1. Introduction

Since the discovery of the open-framework structure alumino-phosphate [1] in 1982, numerous novel metal phosphates with open-framework structures have appeared in the literatures [2], which were synthesized by using organic amines or quaternary ammonium cations as templates. As an alternative approach, organic–inorganic hybrid metal phosphates have been greatly developed by introducing organic component as a ligand [3]. The dramatic expansion of the chemistry of metal phosphates is due to their potential application in the fields of catalysis, adsorption, optical and electromagnetic functional materials [2–5]. The oxovanadium phosphates as an important subclass of this family have been extensively studied [6–18]. Furthermore, associated with the remarkable diversities in the coordination geometry of vanadium in various oxidation states, the secondary metal ions as well as the organic molecules can exert significant influence on the geometric topology of oxovanadium phosphates, a number of bimetallic vanadium phosphate hybrid materials have been reported [19–27]. Bimetallic phosphate means that there are two different transition metals in the phosphate compound, which exhibits special properties not consistent with the properties of the monometallic phosphate. In this field, Zubieta and co-workers have made a prominent contribution. They described a series of oxovanadium phosphates and phosphonates incorporated with a secondary metal atom including 1-D [24,27], 2-D [24–26], and 3-D [26] structures. However, the secondary metal atoms in those complexes reported previously are mainly copper or zinc, the other transition metal oxovanadium phosphates are relatively rare. To our knowledge, only *one* organic–inorganic

---

*Corresponding author. Fax: +86-431-5168624.
E-mail address: wqpang@mail.jlu.edu.cn (W. Pang).

0022-4596/$ - see front matter © 2004 Elsevier Inc. All rights reserved.
doi:10.1016/j.jssc.2004.04.058

hybrid nickel/cobalt–vanadium phosphate has been described in the literature [20]. In order to explore the influence of a secondary metal atom on the framework of the oxovanadium phosphate and provide crystallographic data for mechanism studying further, we have been interested in the syntheses of transition metal oxovanadium phosphates (MVPOs). Here, we report syntheses, structures and magnetic properties of two new layered organic–inorganic hybrid materials $Ni(phen)(H_2O)VO(H_2O)(HPO_4)_2$ **1** and $Co(phen)(H_2O)VO(H_2O)(HPO_4)_2$ **2**.

2. Experimental

2.1. Physical measurements

Powder X-ray (XRD) data were collected on a Siemens D5005 diffractometer with Cu*K*α radiation ($\lambda = 1.5418$ Å). The step size was 0.02° and the count time was 4 s. The elemental analyses (C, H and N) were performed on a Perkin-Elmer 2400 Elemental Analyzer and the inductively coupled plasma (ICP) analyses were conducted on a Perkin-Elmer Optima 3300DV ICP instrument. The infrared (IR) spectra were recorded within the 400–4000 cm^{-1} region on a Nicolet Impact 410 FTIR spectrometer using KBr pellets. Perkin-Elmer TG-7 and DTA-1700 were used to carry out the TGA and DTA analyses in air with a heating rate of 10°C/min.

Magnetic susceptibility data were collected based on a 0.131 and 0.046 g sample of **1** and **2**, respectively over the temperature range 2–300 K at a magnetic field of 5 kG on a Quantum Design MPMS-7 SQUID magnetometer.

2.2. Synthesis

All chemicals purchased were of reagent grade and used without further purification. The title compounds were synthesized in the hydrothermal system. We can get title compounds in a broad range of phen(0.24–0.30 g), but we got big enough crystals suited to be resolved by CCD only in these typical molar ratios. For compound **1**, the starting materials V_2O_5 (0.09 g), Ni $(CH_3COO)_2 \cdot 4H_2O$ (0.25 g), H_3PO_4 (0.24 mL 85 wt%), and 1,10-phen (0.30 g) were dissolved in 5 mL H_2O in the molar ratio of 1:2:7:3:556 and stirred for 90 min. The final reaction mixture was transferred into a 15 mL PTFE lined stainless steel autoclave, and heated at 180°C for 3 d under autogenous pressure. Upon cooling, after filtration, washing and drying in air, green block crystals of **1** were obtained in 70% yield based on vanadium. Anal. found for $C_{12}H_{14}N_2NiO_{11}P_2V$:C, 26.55%; H, 2.66%; N, 5.18%; P, 11.59%; V, 9.38%; Ni, 11.15%; Calc.: C, 26.97%; H, 2.62%; N, 5.24%; P, 11.61%; V, 9.54%; Ni, 10.99%. IR spectrum (cm^{-1}): 3430(br), 1641(s), 1577(w), 1513(m), 1425(s), 1217(w), 1171(m), 1099(m), 1074(m), 1037(m), 943(s), 880(m), 851(m), 727(s), 576(w), 526(s), 434(m). For compound **2**, the starting materials V_2O_5 (0.09 g), $Co(CH_3COO)_2 \cdot 4H_2O$ (0.25 g), H_3PO_4 (0.24mL, 85wt%), and 1,10-phen (0.24 g) were dissolved in 5 mL H_2O in the molar ratio of 1:2:7:2.4:556 and stirred for 90 min. The final reaction mixture was transferred into a 15 mL PTFE lined stainless steel autoclave, and heated at 180°C for 5 d under autogenous pressure. Upon cooling, after filtration washing and drying in air, we got the light red block crystals of **2** in 60% yield based on vanadium. Anal. found for $C_{12}H_{14}N_2CoO_{11}P_2V$: C, 26.04%; H, 2.72%; N, 5.06%; P, 11.67%; V, 9.68%; Co, 10.85%; Calc.: C, 26.96%; H, 2.62%; N, 5.24%; P, 11.61%; V, 9.54%; Co, 11.03%. IR spectrum (cm^{-1}): 3436(br), 1646(s), 1580(m), 1510(m), 1425(s), 1209(w), 1163(m), 1089(m), 1074(m), 1024(m), 943(s), 873(s), 848(m), 727(s), 576(m), 524(s), 434(m).

2.3. X-ray crystallography

Suitable single crystals of the title compound **1** ($0.40 \times 0.35 \times 0.35\ mm^3$) and **2** ($0.25 \times 0.20 \times 0.20\ mm^3$) were selected and mounted on a thin glass fiber, respectively. The intensity data were collected on a Siemens Smart CCD diffractometer equipped with a normal-focus, 2.4 kW sealed-tube X-ray source (graphite-monochromated Mo*K*α radiation, $\lambda(MoK\alpha) = 0.71073$ Å) operating at 50 kV and 40 mA. The number of collected reflections and independent reflections were 7900 and 2346 for **1**, 7935 and 2356 for **2**, respectively. Data processing was accomplished with the SAINT processing program. The structures were solved by direct methods and refined by full-matrix least-squares on F^2 using SHELXTL Version 5.1 [28]. We have introduced the pseudo-orthorhombic twin law [100/0–10/00-1] in the SHELX refinement, and the refined BASF parameter is 0.00134 and 0.00125 for compounds **1** and **2**, respectively. All of the non-hydrogen atoms were refined anisotropically. Hydrogen atoms of aqua ligands were located from difference Fourier maps. Hydrogen atoms from the organic cations and $\{HPO_4\}$ units were located using geometrical constraints.

3. Results and discussion

3.1. Crystal structures

The crystallographic data and details of the data collection and refinement for the structures of **1** and **2** are listed in Table 1. The selected bond lengths and angles are given in Table 2 and 3, respectively. Other

Table 1
Summary of crystal data and structure refinement for **1** and **2**

Compound	**1**	**2**
Empirical formula	$C_{12}H_{14}N_2NiO_{11}P_2V$	$C_{12}H_{14}CoN_2O_{11}P_2V$
Formula weight	533.84	534.06
T (K)	293(2)	293(2)
Crystal system	Monoclinic	Monoclinic
Space group	$P2_1/c$	$P2_1/c$
a (Å)	14.3903(7)	14.3726(4)
b (Å)	15.5232(6)	15.5078(5)
c (Å)	7.3943(3)	7.3932(2)
β (deg)	90.577(2)	90.576(2)
V (Å^3)	1651.7(2)	1647.77(8)
Z	4	4
Dcalc (g cm^{-3})	2.147	2.153
μ (mm^{-1})	1.970	1.838
Reflections collected/ unique	7900/2346 [R(int) = 0.0365]	7735/2356 [R(int) = 0.0387]
Goodness-of-fit on F^2	1.039	1.036
R indices (all data)	$R_1 = 0.0355$, w$R_2 = 0.0776$	$R_1 = 0.0319$, w$R_2 = 0.0629$

Table 2
Selected bond lengths (Å) for compounds **1** and **2**

Compound **1**			
Ni(1)–O(8)	2.020(2)	V(1)–O(4)	2.008(2)
Ni(1)–N(2)	2.066(3)	V(1)–O(6)	2.300(3)
Ni(1)–O(7)	2.077(3)	P(1)–O(1)	1.507(3)
Ni(1)–O(2)#1	2.092(2)	P(1)–O(7)	1.525(3)
Ni(1)–O(9)	2.097(3)	P(1)–O(3)#1	1.527(2)
Ni(1)–N(1)	2.122(3)	P(1)–O(10)	1.596(2)
V(1)–O(2)	1.619(2)	P(2)–O(5)#2	1.517(2)
V(1)–O(1)	1.985(2)	P(2)–O(8)	1.524(2)
V(1)–O(5)	1.993(2)	P(2)–O(4)#3	1.525(2)
V(1)–O(3)	2.001(2)	P(2)–O(11)	1.576(3)
Compound **2**			
Co(1)–O(8)	2.017(2)	V(1)–O(4)	2.0079(19)
Co(1)–N(1)	2.067(3)	V(1)–O(6)	2.298(2)
Co(1)–O(7)	2.071(2)	P(1)–O(1)	1.507(2)
Co(1)–O(9)	2.089(3)	P(1)–O(3)#1	1.520(2)
Co(1)–O(2)#1	2.0934(19)	P(1)–O(7)	1.524(2)
Co(1)–N(2)	2.119 (2)	P(1)–O(10)	1.595(2)
V(1)–O(2)	1.6195(19)	P(2)–O(5)#2	1.519(2)
V(1)–O(1)	1.982(2)	P(2)–O(4)#3	1.520(2)
V(1)–O(5)	1.989(2)	P(2)–O(8)	1.522(2)
V(1)–O(3)	2.0036(19)	P(2)–O(11)	1.578(2)

Symmetry transformations used to generate equivalent atoms: #1 $-x+1,\ -y+1,\ -z+1$; #2 $-x+1,\ y-1/2,\ -z+1/2$; #3 $-x+1,\ -y+1,\ -z$.

Table 3
Selected bond angles (deg) for compounds **1** and **2**

Compound **1**			
O(8)–Ni(1)–N(2)	163.81(10)	O(2)–V(1)–O(4)	96.23(11)
O(8)–Ni(1)–O(7)	101.85(10)	O(1)–V(1)–O(4)	86.46(10)
N(2)–Ni(1)–O(7)	92.92(11)	O(5)–V(1)–O(4)	94.45(9)
O(8)–Ni(1)–O(2)#1	87.24(9)	O(3)–V(1)–O(4)	165.45(10)
N(2)–Ni(1)–O(2)#1	86.51(10)	O(2)–V(1)–O(6)	174.20(11)
O(7)–Ni(1)–O(2)#1	88.64(9)	O(1)–V(1)–O(6)	85.07(11)
O(8)–Ni(1)–O(9)	91.51(13)	O(5)–V(1)–O(6)	77.32(11)
N(2)–Ni(1)–O(9)	96.68(14)	O(3)–V(1)–O(6)	85.26(10)
O(7)–Ni(1)–O(9)	83.86(11)	O(4)–V(1)–O(6)	80.55(10)
O(2)#1–Ni(1)–O(9)	171.98(11)	O(1)–P(1)–O(7)	111.40(14)
O(8)–Ni(1)–N(1)	86.92(10)	O(1)–P(1)–O(3)#1	113.96(14)
N(2)–Ni(1)–N(1)	79.08(11)	O(7)–P(1)–O(3)#1	112.30(14)
O(7)–Ni(1)–N(1)	169.69(10)	O(1)–P(1)–O(10)	106.65(14)
O(2)#1–Ni(1)–N(1)	97.27(10)	O(7)–P(1)–O(10)	107.91(14)
O(9)–Ni(1)–N(1)	90.57(12)	O(3)#1–P(1)–O(10)	104.01(13)
O(2)–V(1)–O(1)	99.61(11)	O(5)#2–P(2)–O(8)	111.57(14)
O(2)–V(1)–O(5)	98.21(11)	O(5)#2–P(2)–O(4)#3	111.97(13)
O(1)–V(1)–O(5)	161.95(11)	O(8)–P(2)–O(4)#3	108.97(13)
O(2)–V(1)–O(3)	98.17(11)	O(5)#2–P(2)–O(11)	109.75(13)
O(1)–V(1)–O(3)	89.16(10)	O(8)–P(2)–O(11)	105.02(13)
O(5)–V(1)–O(3)	85.49(9)	O(4)#3–P(2)–O(11)	109.31(14)
Compound **2**			
O(8)–Co(1)–N(1)	163.65(9)	O(2)–V(1)–O(4)	96.23(9)
O(8)–Co(1)–O(7)	101.83(8)	O(1)–V(1)–O(4)	86.38(8)
N(1)–Co(1)–O(7)	93.10(9)	O(5)–V(1)–O(4)	94.44(8)
O(8)–Co(1)–O(9)	91.40(10)	O(3)–V(1)–O(4)	165.46(8)
N(1)–Co(1)–O(9)	96.80(11)	O(2)–V(1)–O(6)	174.08(10)
O(7)–Co(1)–O(9)	84.02(9)	O(1)–V(1)–O(6)	84.96(9)
O(8)–Co(1)–O(2)#1	87.29(8)	O(5)–V(1)–O(6)	77.44(9)
N(1)–Co(1)–O(2)#1	86.45(9)	O(3)–V(1)–O(6)	85.40(8)
O(7)–Co(1)–O(2)#1	88.59(8)	O(4)–V(1)–O(6)	80.40(8)
O(9)–Co(1)–O(2)#1	172.07(9)	O(1)–P(1)–O(3)#1	114.16(11)
O(8)–Co(1)–N(2)	86.91(9)	O(1)–P(1)–O(7)	111.36(13)
N(1)–Co(1)–N(2)	78.92(9)	O(3)#1–P(1)–O(7)	112.21(11)
O(7)–Co(1)–N(2)	169.79(9)	O(1)–P(1)–O(10)	106.72(12)
O(9)–Co(1)–N(2)	90.55(10)	O(3)#1–P(1)–O(10)	103.97(11)
O(2)#1–Co(1)–N(2)	97.19(8)	O(7)–P(1)–O(10)	107.82(11)
O(2)–V(1)–O(1)	99.75(10)	O(5)#2–P(2)–O(4)#3	111.89(11)
O(2)–V(1)–O(5)	98.07(9)	O(5)#2–P(2)–O(8)	111.76(11)
O(1)–V(1)–O(5)	161.97(9)	O(4)#3–P(2)–O(8)	109.25(12)
O(2)–V(1)–O(3)	98.18(9)	O(5)#2–P(2)–O(11)	109.39(12)
O(1)–V(1)–O(3)	89.26(8)	O(4)#3–P(2)–O(11)	109.20(11)
O(5)–V(1)–O(3)	85.49(8)	O(8)–P(2)–O(11)	105.11(11)

Symmetry transformations used to generate equivalent atoms: #1 $-x+1,\ -y+1,\ -z+1$; #2 $-x+1,\ y-1/2,\ -z+1/2$; #3 $-x+1,\ -y+1,\ -z$.

crystallographic data in details are given in the supporting information.

Single crystal X-ray diffraction analyses reveal that compounds **1** and **2** are isostructural [29] and crystallize in the monoclinic system with $P2_1/c$ space group. Here we describe the structure of compound **1** as a representative. Compound **1** consists of a novel 2-D layer capped by $[Ni(phen)]^{2+}$ complexes with phen groups projecting above and below into the interlamellar regions. The asymmetric unit of structure is shown in Fig. 1. The Ni atom is six-coordinated by two nitrogen atoms from a phen ligand, two oxygen atoms from two $\{HPO_4\}$ units, one oxygen atom of aqua ligand, and one oxygen briging to $\{VO_6\}$ octahedron. The octahedral coordination about V atom is defined by four oxygen atoms from four $\{HPO_4\}$ units in the basal plane, one oxygen atom from aqua ligand, and one oxygen atom

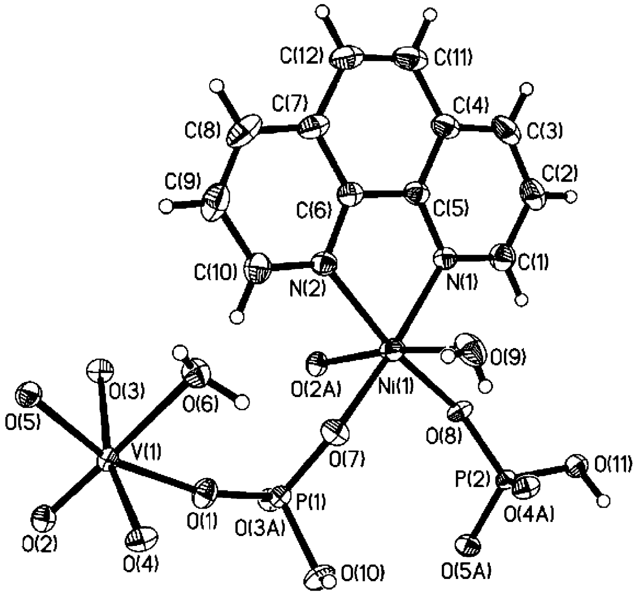

Fig. 1. ORTEP view of the coordination environments of the nickel, vanadium, and phosphorus atoms in **1**, showing the atom labeling scheme and 50% thermal ellipsoids.

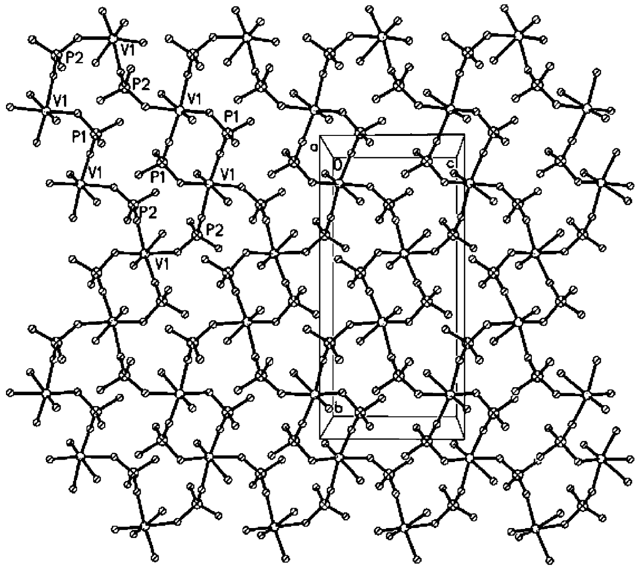

Fig. 2. The V–P–O layer of **1** viewed along the *a*-axis.

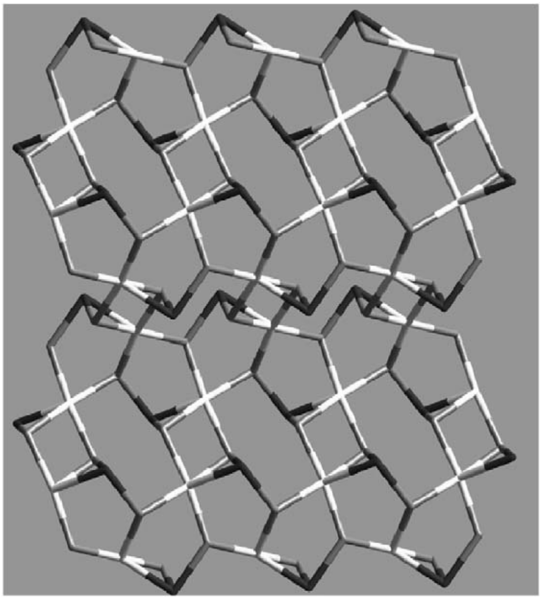

Fig. 3. View of the Ni/V/P/O layer in the *bc*-plane of **1**, showing 3, 4, 5, 8-member rings.

corner-shared with $\{NiO_4N_2\}$ octahedron. The oxo-bridge connecting V and Ni is asymmetric with a V–O bond distance of 1.619(2) Å and Ni–O distance of 2.092(2) Å. The two phosphorous atoms are each coordinated by a terminal {OH} (O–H distances is 0.8200 Å) group and three oxygen atoms of which two are shared with two $\{VO_6\}$ octahedra and one is shared with the $\{NiO_4N_2\}$ octahedron. The P–O distance range from 1.507(3) to 1.596(2) Å and the O–P–O angles lie between 104.0(2)° and 114.0 (2)°. The bond valence sum calculations [30], giving oxidation states of corresponding ions, indicate the occurrence of $Ni^{2+}(Co^{2+})$, V^{4+} and P^{5+}.

A view along the *a*-axis to the 2D (V–P–O) layer, is shown in Fig. 2. The layer structure of **1** is built up from a strictly alternating $\{VO_6\}$ octahedra and $\{HPO_4\}$ tetrahedra sharing vertices forming the common 4-membered ring $\{V_2P_2O_4\}$, which have been observed previously [27]. Then four such 4-membered rings are linked through four P(2) sites forming a 12-membered ring $\{V_6P_6O_{12}\}$, the consequence of the connectivity results in an undulating layer. It is noteworthy that the $\{NiO_4N_2\}$ octahedra which are connected to two P and one V atoms of the V–P–O 4,12-rings capped up and down the layers, thereby forming a new Ni–V–P–O layer which is composed of 3,4,5,8-membered rings. Because of the up- and down-capped $\{NiO_4N_2\}$ octahedra to the V–P–O layers, the former V–P–O 12-rings are each changed into two 5-rings and one 8-ring, as shown in Fig. 3. To our knowledge, such an inorganic oxovanadium phosphate backbone capped by the transition metal complexes has not been observed before. It is also striking that the phen groups projecting into the interlamellar regions orientated in two directions at a dihedral of 48.9°. Finally, it should be noted that the phen groups projecting from the adjacent layers interdigitate and provide a strong $\pi-\pi$ stacking interaction (ca. 3.35 or 3.39 Å interplanar separations) [31], which make the neighboring layers stably packed together. The bimetallic phosphate undulating layers, therefore, extend into 3-D supermolecular arrays, as shown in Fig. 4. The weak intralayer hydrogen bonding interactions also perform a certain function on stabilizing the wave-like layer structure of **1**.

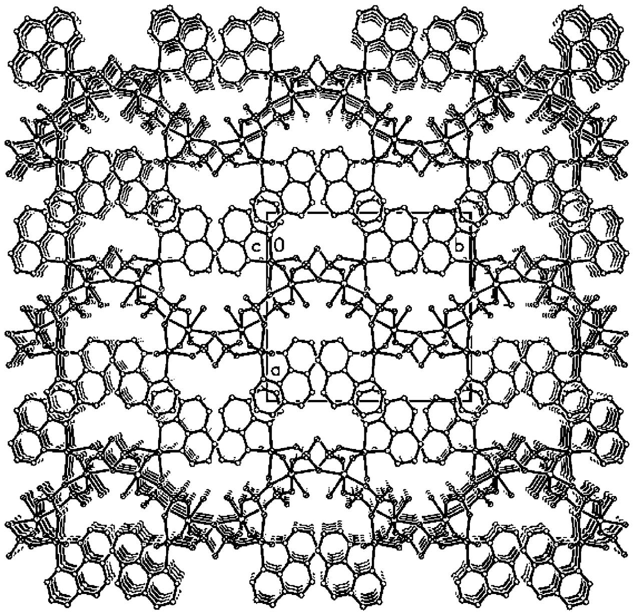

Fig. 4. View along the *c*-axis, showing the 3D supermolecular structure of **1**.

3.2. Thermal analyses

The TG curves of the two compounds can be divided into three weight losses steps. The first, which occur in the range of 170–420°C for **1** (180–410°C for **2**), is attributed to the removal of H_2O coordinated to V and Ni (Co) atoms and H_2O from $\{HPO_4\}$ groups [15,32]. The observed weight loss 9.56% for **1** (10.72% for **2**) is agreement with the calculated value 10.11%. The second weight loss is 6.64% for **1** (5.86% for **2**) in the temperature range 420–523°C (410–570°C for **2**). The third weight loss is 25.83% from 523 to 760°C for **1** (26.45% from 570 to 900°C for **2**). These two continuous weight losses are ascribed to the release of phen groups [33,34], which may be due to the decomposition of phen groups by stages, but they are not exhibiting well-defined intermediate products. The whole weight loss 42.58% for **1** (43.03% for **2**) is in agreement with the calculated value 43.83%. The sample does not lose weight at temperature higher than 760°C (900°C for **2**).

3.3. Magnetic properties

The temperature dependent susceptibility data of compounds **1** and **2** have been measured in the range 300–2 K. Figs. 5 and 6 show the plots of the χ_M and $\chi_M T$ vs. T curves for **1** and **2**, respectively. The χ_M vs. T plots show typical Curie–Weiss behavior. The susceptibility data can be fitted to the Curie–Weiss law $\chi_M = C_M/(T—\theta)$, where C is the Curie constant, T the temperature and θ the Weiss constant. The best Non-linear curve fitting to the susceptibility data yields the

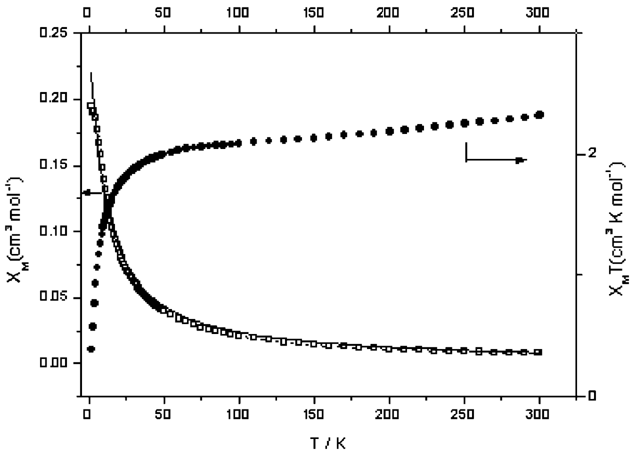

Fig. 5. χ_M and $\chi_M T$ vs. T plots for compound **1**.

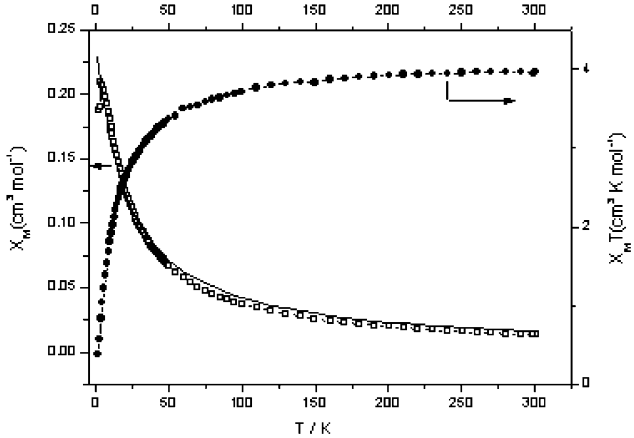

Fig. 6. χ_M and $\chi_M T$ vs. T plots for compound **2**.

$C_M = 2.58\,\mathrm{cm^3\,K/mol}$ and $\theta = -9.73\,\mathrm{K}$ of **1** and $C_M = 5.00\,\mathrm{cm^3\,K/mol}$ and $\theta = -19.87\,\mathrm{K}$ of **2**. Which indicate that the dominant magnetic exchange interactions are antiferromagnetic in origin. These are further confirmed by the continuous decrease in the quantity $\chi_M T$ with decreasing temperature. At 300 K, the calculated effective magnetic moments, determined from the equation $\mu_{\mathrm{eff}} = 2.83(\chi_M T)^{1/2}$, are $4.30\,\mu_B$ for **1** and $5.63\,\mu_B$ for **2**, which were higher than those expected spin-only moment for such combinations calculated to be $3.32\,\mu_B$ for **1** and $4.24\,\mu_B$ for **2** (according to the formula $\mu = [n(n+2) + m(m+2)]^{1/2}$ where n and m are the numbers of unpaired electron each center), possibly due to the significant orbital contribution of the magnetic centers. The magnetic behavior of compounds **1** and **2** is consistent with the fact that there are two different paramagnetic metal ions, Ni(Co) (II) and V(IV), with dissimilar g values. Taking the structure of **1** into consideration, there are two super-exchange pathways in the layers: one is through O–P–O and the other is through one oxygen bridge. Intralayer metal–metal (Ni–Ni, Ni–V, V–V) distance are in the range

3.5043–7.9709 Å. The Ni–V and V–V distance are shorter than that of the similar compound [Cu(phen)(VO)($O_3PCH_2PO_3$)(H_2O)] [26], so some interactions may be expected although the true magnetic dimensionality is not entirely clear.

4. Conclusion

In summary, we have successfully prepared two new bimetallic phosphate organic–inorganic hybrid materials, which have an undulating inorganic V–P–O layer consists of 4,12-membered rings capped by $[M(\mathrm{phen})]^{2+}$ ($M=$ Ni, Co) complexes with phen projecting below and above the interlameller regions. These layers extend into 3D supermolecular arrays through $\pi-\pi$ stacking interactions between interlayer phen groups. Extended researches are underway to reveal the synthetic rules and explore their attractive properties.

5. Supplementary material

Crystallographic data for the structure of the compounds reported in this paper have been deposited in the Cambridge Crystallographic Data center as supplementary publication number CCDC 215477 & 215478. Copies of the data can be obtained free of charge on application to CCDC, 12 Union Road, Cambridge CB21EZ, UK (fax: (+44)1223-336-033; e-mail: deposit@ccdc.com.ac.uk).

Acknowledgments

The authors acknowledge the financial support of the State Basic Research Project of China (G200077507), the National Natural Science Foundation of China (20233030), and the State Key Laboratory of Inorganic Synthesis and Preparative Chemistry of Jilin University.

References

[1] S.T. Wilson, B.M. Lok, C.A. Messina, T.R. Cannan, E.M. Flanigen, J. Am. Chem. Soc. 104 (1982) 1146.
[2] A.K. Cheetham, G. Ferey, T. Loiseau, Angew. Chem., Int. Ed. 38 (1999) 3268 and references therein.
[3] P.J. Hagrman, D. Hagrman, J. Zubieta, Angew. Chem., Int. Ed. 38 (1999) 2638 and references therein.
[4] G. Ferey, Chem. Mater. 13 (2001) 3084 and references therein.
[5] M. Eddaoudi, D.B. Moler, H. Li, B. Chen, T.M. Reineke, M. O'Keeffe, O.M. Yaghi, Acc. Chem. Res. 34 (2001) 319 and references therein.
[6] V. Soghomonian, Q. Chen, R.C. Haushalter, J. Zubieta, C.J. O'Connor, Science 259 (1993) 1596.
[7] V. Soghomonian, Q. Chen, R.C. Haushalter, J. Zubieta, Angew. Chem. Int. Ed. Engl. 32 (1993) 610.
[8] V. Soghomonian, Q. Chen, R.C. Haushalter, J. Zubieta, C.J. O'Connor, Y.S. Lee, Chem. Mater. 5 (1993) 1690.
[9] T. Loiseau, G. Ferey, J. Solid State Chem. 111 (1994) 416.
[10] X. Bu, P. Feng, G. Stucky, J. Chem. Soc., Chem. Commun. (1995) 1337.
[11] W.T.A. Harrison, K. Hsu, A.J. Jacobson, Chem. Mater. 7 (1995) 2004.
[12] D. Riou, F. Taulelle, G. Ferey, Inorg. Chem. 35 (1996) 6392.
[13] J. Do, R.P. Bontchev, A.J. Jacobson, J. Solid State Chem. 154 (2000) 514.
[14] C.-H. Huang, L.-H. Huang, K.-H. Lii, Inorg. Chem. 40 (2001) 2625.
[15] Y. Lu, E.-B. Wang, M. Yuan, G.-Y. Luan, Y.-G. Li, H. Zhang, C.-W. Hu, Y.-G. Yao, Y.-Y. Qin, Y.-B. Chen, J. Chem. Soc., Dalton Trans. (2002) 3029.
[16] W.T.A. Harrison, Solid State Sci. 5 (2003) 297.
[17] C. Qin, L. Xu, Y. Wei, X. Wang, F. Li, Inorg. Chem. 42 (2003) 3107.
[18] N. Calin, C. Serre, S.C. Sevov, J. Mater. Chem. 13 (2003) 531.
[19] M. Roca, M.D. Marcos, P. Amorüs, A.B. Beltrán-Porter, A.J. Edwards, D.B. Beltrán-Porter, Inorg. Chem. 35 (1996) 5631.
[20] Z. Shi, S.-H. Feng, S. Gao, L.-R. Zhang, G.-Y. Yang, J. Hua, Angew. Chem. Int. Ed. 39 (2000) 2325.
[21] Z. Shi, S.-H. Feng, L.-R. Zhang, G.-Y. Yang, J. Hua, Chem. Mater. 12 (2000) 2930.
[22] X.-M. Zhang, M.-L. Tong, S.-H. Feng, X.-M. Chen, J. Chem. Soc., Dalton Trans. (2001) 2069.
[23] C.-M. Wang, K.-H. Lii, J. Solid State Chem. 172 (2003) 194.
[24] R. Finn, J. Zubieta, J. Chem. Soc., Chem. Commun. (2000) 1321.
[25] R. Finn, J. Zubieta, J. Chem. Soc., Dalton Trans. (2000) 1821.
[26] R. Finn, R. Lam, J. Greedan, J. Zubieta, Inorg. Chem. 40 (2001) 3745.
[27] R.C. Finn, J. Zubieta, J. Chem. Soc., Dalton Trans. (2002) 856.
[28] G.M. Sheldrick, SHELXL-97, Program for Refinement of Crystal Structures, University of Göttingen, Germany, 1997.
[29] J. Lima-de-Faria, E. Hellner, F. Liebau, E. Makovicky, E. Parth, Acta Crystallogr. A 46 (1990) 1–11.
[30] I.D. Brown, D. Altermatt, Acta Crystallogr. B 41 (1985) 244.
[31] S.B. Ferguson, E.M. Sanford, E.M. Seward, F. Diederich, J. Am. Chem. Soc. 113 (1991) 5410.
[32] Y.-M. Tsai, S.-L. Wang, C.-H. Huang, K.-H. Lii, Inorg. Chem. 38 (1999) 4183.
[33] Y.-G. Li, G.-J. De, M. Yuan, E.-B. Wang et al., Dalton Trans. (2003) 331.
[34] D.-R. Xiao, Y. Lu, E.-B. Wang, et al., J. Solid State Chem. 175 (2003) 146.